Hydrogen Exchange Kinetics of RNase A and the Urea:TMAO Paradigm[†]

Youxing Qu and D. Wayne Bolen*

Department of Human Biological Chemistry and Genetics, University of Texas Medical Branch, 5.154 MRB, Galveston, Texas 77555-1052

Received November 5, 2002; Revised Manuscript Received March 24, 2003

ABSTRACT: A key paradigm in the biology of adaptation holds that urea affects protein function by increasing the fluctuations of the native state, while trimethylamine *N*-oxide (TMAO) affects function in the opposite direction by decreasing the normal fluctuations of the native ensemble. Using urea and TMAO separately and together, hydrogen exchange (HX) studies on RNase A at pH* 6.35 were used to investigate the basic tenets of the urea:TMAO paradigm. TMAO (1 M) alone decreases HX rate constants of a select number of sites exchanging from the native ensemble, and low urea alone increases the rate constants of some of the same sites. Addition of TMAO to urea solutions containing RNase A also suppresses HX rate constants. The data show that urea and TMAO independently or in combination affect the dynamics of the native ensemble in opposing ways. The results provide evidence in support of the counteraction aspect of the urea:TMAO paradigm linking structural dynamics with protein function in urea-rich organs and organisms. RNase A is so resistant to urea denaturation at pH* 6.35 that even in the presence of 4.8 M urea, the native ensemble accounts for >99.5% of the protein. An essential test, devised to determine the HX mechanism of exchangeable protons, shows that over the 0−4.8 M urea concentration range nearly 80% of all observed sites convert from EX2 to EX1. The slow exchange sites are all EX1; they do not exhibit global exchange even at urea concentrations (5.8 M) well into the denaturation transition zone, and their energetically distinct activated complexes leading to exchange gives evidence of residual structure. Under these experimental conditions, the use of ΔG_{HX} as a basis for HX analysis of RNase A urea denaturation is invalid.

Certain plants, animals, and microorganisms have adapted to environmental stresses that bring about changes in water activity within the cells of these organisms (*1*). The mechanism of this adaptation involves the intracellular accumulation of small organic molecules known as organic osmolytes (*2*). In addition to helping alleviate the water stress, many of the organic osmolytes stabilize proteins and other cellular components against denaturing stresses that often accompany the environmental condition. Remarkably, these osmolytes provide such stabilization without substantively altering the functional properties of the proteins with which they are in contact (*2*−*4*). Some protecting osmolytes have been classified as "compatible osmolytes" in recognition of their rather innocuous effects on macromolecular and cellular function (*3*, *5*−*7*). An adaptation that provides protection against water stress and denaturing stresses without altering cellular processes presents a strong selective advantage to the organism in adapting to the new environment.

An additional group of protecting organic osmolytes, classified as "counteracting", has been identified in organisms and organs that accumulate significant intracellular concentrations of urea (*8*). In the urea-rich elasmobranchs (sharks and rays) and in mammalian organs such as kidney, urea is present at sufficient intracellular concentrations to alter functional and in some cases structural properties of intracellular proteins (*8*−*14*). Protecting osmolytes are also present in these cases, and are classified as "counteracting osmolytes" because of their ability to stabilize proteins against the denaturing effects of urea while also affecting protein function in a manner opposite to that of urea (*8*, *15*). By way of example, urea often affects enzyme function by decreasing k_{cat} values and increasing K_m values (*11*). By contrast, counteracting osmolytes such as trimethylamine *N*-oxide (TMAO)[1] tend to increase k_{cat} and decrease K_m values (*10*). Alone or in combination, urea and TMAO generally have opposite effects on protein function. In urea-rich organisms such as sharks and rays the ratio of urea:TMAO is around 2:1 or 3:2 (*2*). With many (but not all) enzymes that have been studied, the k_{cat} and K_m values in the presence of a 2:1 or 3:2 urea:TMAO are essentially the same as the k_{cat} and K_m values observed for the same enzymes in the absence of both osmolytes (*11*, *16*, *17*) (see review by Yancey (*18*)). Understanding the molecular basis of TMAO counteraction of urea effects on enzyme function is an important aspect of understanding biological adaptation and the possible roles of organic osmolytes in kidney.

Mashino and Fridovich presented a plausible molecular-level explanation to the paradigm of how urea alone might increase the K_m of an enzyme, how TMAO alone would decrease it, and how the correct urea:TMAO ratio could

[†] Support provided by NIH Grant GM49760 (to D.W.B.).

* Corresponding author e-mail: wbolen@hbcg.utmb.edu; (409) 772−0754; (409) 747−4751 (fax).

[1] Abbreviations: TMAO, trimethylamine-*N*-oxide; RNase A, ribonuclease A; NMR, nuclear magnetic resonance; HX, hydrogen exchange; pH*, uncorrected pH meter reading in D_2O; GdnHCl, guanidine hydrochloride; 2D-COSY, two-dimensional homonuclear correlation spectroscopy; H/D, hydrogen−deuterium.

10.1021/bi0206457 CCC: $25.00
Published on Web 04/26/2003

Scheme 1

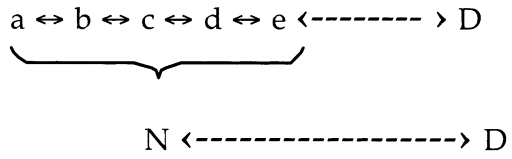

result in TMAO counteracting the effects of urea (*19*). They considered the native state (N) of an enzyme as composed of an ensemble of microstates a, b, c, d and e, with "a" being the most compact species and "e" being the least compact (Scheme 1, with D as the denatured state). For purposes of illustration, let us assume that the microspecies have a gradation of affinities for substrate, with "a" having the highest affinity and "e" having the least. It is further assumed that in buffer solution alone microstate "c" is the predominant species, and the observed substrate binding constant is an average quantity with a magnitude close to that expected for species "c" alone. Mashino and Fridovich expected TMAO and urea to influence the distribution of microstates in defined and opposing manners, with urea shifting the ensemble in the direction of less compact species while TMAO shifts it toward the more highly compact microstates. This set of assumptions applied to the above model should result in an increased enzyme K_m in the presence of urea alone, a decreased K_m in the presence of TMAO alone, and a K_m in the presence of TMAO plus urea that is similar to that observed in the absence of both osmolytes (*19*). Their model, which we refer to as the urea:TMAO paradigm, also can explain exceptions to the functional behavior of urea and TMAO as has sometimes been observed (*19*, *20*).

It has long been thought that the kinetic parameters, K_m and k_{cat}, depend on fluctuations of the native state, but the details of how structural fluctuations are connected with protein function are unclear (*21*, *22*). From an experimental standpoint, what is most attractive about the molecular-level model as described by the urea:TMAO paradigm is that it postulates the ensemble nature of the native state as the basis for explaining the origin of observed K_m effects, thereby relating structural dynamics to protein function. From what is known concerning the osmophobic effect, it is reasonable to expect that TMAO should promote more compact, and urea less compact protein species (*23*). Thus, the model provides a prediction that appears to be testable by means of existing experimental techniques. Finally, if the model is correct, the well-documented counteraction of urea effects on protein structure and function by TMAO can be readily appreciated.

Here, we explore the effects of urea, TMAO, and urea:TMAO mixtures on the hydrogen−deuterium (H/D) exchange kinetics of amide protons of the native state ensemble of ribonuclease A (RNase A). Because site-specific amide proton exchange arises from protein structural fluctuations, H/D exchange kinetics opens possibilities for determining whether TMAO and/or urea alter the ensemble of microstates that comprise the native protein. It is known that very high concentrations of urea are needed to denature RNase A (*24*). As detected by hydrogen exchange (HX), the resistance of RNase A to urea denaturation permits native state protein fluctuations to be studied over a much larger denaturant concentration range than previously attempted.

MATERIALS AND METHODS

RNase A (E.C. 2.7.7.17, lot 88871) was purchased from ICN Biomedicals Inc. Ultrapure urea (lot M7B1237) was obtained from Nacalai Tesque, Inc., Kyoto, Japan, TMAO (>99%), imidazole (>99.5%), and glycinamide hydrochloride (>99%) were from Fluka company, and all deuterated reagents, including D_2O (99.96% D), D_3PO_4 (85%), DCl (20%), and NaOD (30%), were from Cambridge Isotope Laboratories, Inc.

Hydrogen exchange of RNase A was conducted in nine urea concentrations in the absence of TMAO, and in six urea concentrations in the presence of 1 M TMAO. All the hydrogen exchange experiments were performed at 25 °C and pH* 6.35 (uncorrected pH meter reading). An additional experiment in 4.8 M urea was performed at pH* 7.05 for the purpose of conducting the EX2/EX1 test. Urea and TMAO concentrations were evaluated by refractometry using the equations:

$$[\text{urea}] = 117.66^*\Delta n + 29.753^*\Delta n^2 + 185.56\,\Delta n^3$$

$$[\text{TMAO}] = -0.0038 + 103.3151^*\Delta n - 259.43^*\Delta n^2$$

where Δn is the refractive index difference between urea or TMAO solutions and the corresponding D_2O buffers in which they were prepared (*25*, *26*). For the mixture of urea plus 1 M TMAO solution, urea and TMAO solutions were prepared separately at 2× desired concentration and then mixed 1:1, with pH readjusted after mixing. Imidazole (0.1 M) was used as buffer, and 0.1 M glycinamide hydrochloride was also added to take up the cyanate from the decomposition of urea. At pH* 6.35, the main reaction of cyanate with RNase A is the carbamoylation of the unprotonated amino groups (*27*). This reaction is highly dependent on the pK_a of the amine. Because of their lower pK_a values, at neutral pH α-amino groups react almost 100-fold more rapidly than do ϵ-amino groups (*28*). The addition of glycinamide hydrochloride (pK_a = 8.1) in high concentration (0.1 M) protects the ϵ-amino groups of Lys residues (pK_a = 10.5) and the N-terminal α-amino group of the protein from modification by cyanate.

Typically for a hydrogen exchange experiment, 500 mg of RNase A was dissolved in 10 mL of water, pH was adjusted to 6.35, and the protein solution was lyophilized. To initiate hydrogen exchange, the lyophilized protein powder was dissolved in 10 mL of urea or urea + 1 M TMAO solution prepared in buffered D_2O, giving a pH* of 6.35 after mixing. Volume increase by the addition of RNase A was considered, and a specific volume of 0.70 mL/g was used for RNase A. The reported urea ±1 M TMAO concentrations were corrected for volume change. Because high concentrations of nondeuterated buffered TMAO and/or urea were used, we avoided their contributions to the protein NMR signal by adopting the quench method described in Wang et al. (*29*). At given times after dissolving RNase A in the osmolyte solutions, aliquots of 0.5 mL were taken from the HX reaction and applied to a Pharmacia Hitrap desalting column, equilibrated, and eluted with pH* 3.0, 50 mM phosphate buffer in D_2O. In this way, the protein was separated from additives (urea, TMAO, imidazole, glycinamide hydrochloride) and exchange was quenched by dropping pH* to 3.0. The separation procedure took only 1 ∼ 2 min, and the protein concentration was diluted about

2-fold as a result of the chromatography. The final protein concentration for NMR was about 1 ~ 2 mM. The quenched sample was immediately frozen in dry ice/ethanol bath and kept at −20 °C. Sample solutions were thawed just before NMR measurement at pH* 3. A critical difference between the current experiments and those reported previously by this laboratory is the absence of azide in the current experiments (*29*). After the previous studies, we found that azide can greatly affect the HX rate constants at many amide sites. Because of this, the EX1/EX2 test described below should not be applied to the data reported previously.

Two-dimensional COSY NMR was used for measurements of exchange rate constants. All experiments were run at 35 °C on a Varian Unity Plus 600 MHz spectrometer, and the NMR data were processed with Varian VNMR software. For each COSY, the spectral width was 7200 Hz, and eight scans were collected for each data point. The COSY experiment took about 1 h per sample. Acquisition of 4096 and 256 data points in the t2 and t1 time domains occurred, and prior to Fourier transformation 1D data were zero-filled to 4096 points in t1 dimension. Unshifted sine bell window function was applied in both dimensions.

The COSY peak assignments were easily made by comparison with the literature (*30*, *31*). To evaluate the rate constant of each residue, the volume or height of the NH−C−H cross-peak was first normalized to that of the nonexchanging Tyr25 ring proton cross-peak, then the normalized ratio was fitted to a single-exponential function $A = A_0[\exp(-k_{ex}t)] + C$, where C is a constant.

The effects of various concentrations of urea and/or 1 M TMAO on the intrinsic H/H chemical exchange rate constants of PDLA and the tetrapeptide AGSE were measured on a 600 MHz NMR spectrometer at 25 °C using saturation transfer technique (*32*−*34*). This method was described previously (*29*). A low-power solvent preirradiation time of 3 s was used in all experiments and the total recycle delay was 9 s. T_1 was measured by the inversion−recovery method. The intrinsic chemical exchange rate constant (k_{int}) was calculated from the equation:

$$I/I_0 = 1/(1+ k_{int}T_1)$$

Here, I represents the normalized NH peak intensity (normalized to the methyl peak intensity of AGSE) at the test pH, and I_0 was the normalized NH peak intensity around pH 3 where exchange is at its minimum.

Urea unfolding experiments of RNase A were performed under the same conditions used for hydrogen exchange (25 °C, pH* 6.35 and 7.05, 0.1 M imidazole, and 0.1 M glycinamide buffer in 99.96% D_2O), following the method of Yao and Bolen (*24*). Deuterated urea was made by lyophilization in D_2O and was further purified by Bio-Rad mix-bed ion-exchange resin AG501-X8. The unfolding was monitored by absorbance at 287 nm using an Aviv UV spectrometer fitted with a pair of matched 1-cm quartz cuvettes with screw caps. For each data point, an aliquot of solution was removed from the sample cuvette, the same volume of 10 M urea stock solution was added with stirring, and the absorbance was measured. Complete mixing was achieved by magnetic stirring for about 2 min. As indicated by no further change of absorbance with time, equilibrium denaturation was reached 10−30 min after addition of urea.

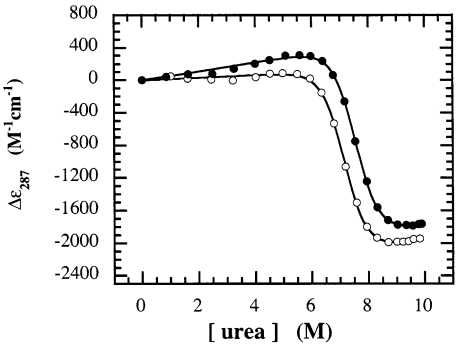

FIGURE 1: Urea-induced equilibrium denaturation of RNase A at 25 °C, in D_2O containing 0.1 M imidazole, 0.1 M glycinamide at pH* 6.35 (open circles) and pH* 7.05 (filled circles). Denaturation was monitored using the extinction coefficient difference at 287 nm.

Table 1: Thermodynamic Parameters of RNase A Urea-Induced Unfolding in Buffered D_2O at 25 °C

pH*	$\Delta G^\circ_{N\rightarrow D}$ kcal/mol	m kcal/mol × M^{-1}	$C_{1/2}$ M	ΔG (4.8 M urea) kcal/mol
6.35	10.66 ± 0.40	1.49 ± 0.06	7.16	3.52 ± 0.29
7.05	10.93 ± 0.39	1.45 ± 0.05	7.59	3.97 ± 0.24

The unfolding data were fitted to a two-state model using the method previously developed in this laboratory (*35*).

RESULTS

To establish the urea concentration range over which the native ensemble of RNase A is the dominant species, equilibrium denaturation measurements were carried out at 25 °C in buffered D_2O at pH* 6.35 and 7.05, giving the results shown in Figure 1. Nonlinear least-squares fitting of these data to the linear extrapolation model yields the denaturation change in Gibbs energy in the limit of zero denaturant concentration, along with m values shown in Table 1. It is clear from the denaturation Gibbs energy changes at the pH* values reported in Table 1 that the population of native RNase A is greater than 99.5% in 4.8 M urea. Thus, we can be assured that by staying within the concentration range of 0−4.8 M urea, the native state of RNase A will be the dominant protein species present in evaluating H/D exchange kinetics.

In the presence of organic osmolytes, H/D exchange rate constants could be affected by a number of factors. In the present study, a basic question is whether the organic osmolytes affect H/D rate constants of fully solvent-exposed amide protons. It has long been known that urea diminishes intrinsic rate constants for amide H/D exchange (*36*, *37*), and Figure 2 shows that the intrinsic rate constant for the glycine amide proton of the AGSE tetrapeptide is decreased by 2−2.5-fold in 4 M urea. These results are consistent with a 5-fold decrease in HX rate constants of model compound amide protons in 8 M urea noted by Loftus et al. (*37*).

In contrast to urea, the effect of 1 M TMAO on intrinsic H/D exchange of fully exposed amide protons is found to be negligible or nonexistent (see Figure 2). Furthermore, kinetic data collected in the combined presence of 1 M TMAO and 4 M urea (Figure 2) show that TMAO does not alter the H/D exchange rate constant from that caused by 4 M urea alone. H/D exchange kinetics on tetrapeptides of different sequences have also been investigated, giving results such

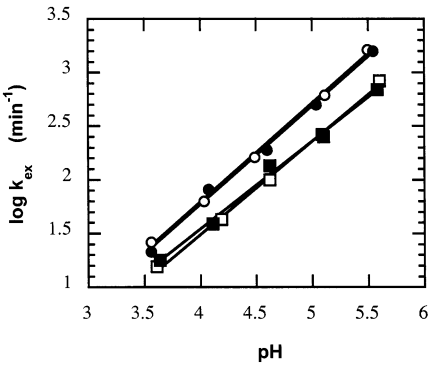

FIGURE 2: Intrinsic HX rate constants of the glycine amide proton of the tetrapeptide, AGSE as a function of pH*. Performed in 50 mM citric acid buffer (open circles), in buffered 1 M TMAO (filled circles), in buffered 4 M urea (open squares), and in buffered 4 M urea plus 1 M TMAO (filled squares). Individual linear least-squares fits of each data set are shown.

as that shown in Figure 2. Accordingly, TMAO is considered to be unperturbing in its effects on fully solvent-exposed amide protons either by itself, or in combination with urea.

H/D exchange rate data are most commonly discussed and interpreted in terms of the general model (eq 1) for protein hydrogen exchange (*38*).

$$\text{(closed)} \underset{k_{cl}}{\overset{k_{op}}{\rightleftharpoons}} \text{(open)} \xrightarrow{k_{ch}} \text{exchange} \qquad (1)$$

Near neutral pH, most native state amide protons are buried in the protein interior and are often hydrogen bonded. These amide protons are considered to be in a " closed " solvent-inaccessible state and are exchange incompetent. By means of some fluctuation(s) or solvent penetration event, an amide proton in the "closed" state becomes "open" (solvent exposed), at which point exchange may occur by the deuterioxide-dependent reaction with the chemical rate constant, k_{ch}.

For this general kinetic mechanism, the observed rate constant k_{ex} is given by

$$k_{ex} = \frac{k_{op}k_{ch}[OD^-]}{k_{cl} + k_{ch}[OD^-]} \qquad (2)$$

where k_{op} and k_{cl} are the rate constants for the opening and closing event or fluctuation, and k_{ch} is the rate constant for exchange of an exposed amide site (*36*).

Two limiting mechanisms, EX1 and EX2, arising from the relative values of k_{ch}, k_{op}, and k_{cl}, may occur for this mechanism.

$$\text{EX1: If } k_{ch}[OD^-] >> k_{cl}, \text{ then } k_{ex} = k_{op} \qquad (3)$$

$$\text{EX2: If } k_{ch}[OD^-] << k_{cl} \text{ then } k_{ex} = (k_{op}/k_{cl})k_{ch}[OD^-] = K_{op}k_{ch}[OD^-] \qquad (4)$$

$$K_{op} = k_{op}/k_{cl} \qquad (5)$$

where K_{op} is the equilibrium constant of the opening event for that amide proton under EX2 conditions, and the apparent hydrogen exchange free energy (ΔG_{HX}) can be determined from eq 6, provided k_{ch} [OD$^-$] is known from model studies (*39*) and k_{ex} is evaluated from kinetic data. Within the pH* range of 6.3−7 and 25 °C, it is common to assume that protein H/D exchange occurs by the EX2 mechanism, but at higher pH*, higher temperature, or if denaturant is present, it is possible for the mechanism to shift from EX2 to EX1 (*40*−*45*).

$$\Delta G_{HX} = -RT \ln K_{op} = RT \ln(k_{ch}[OD^-]/k_{ex}) \qquad (6)$$

Test for EX1 and EX2. With knowledge that RNase A is greater than 99.5% native in 4.8 M urea concentrations at pH* 6.35 and 7.05, a test can be performed in the presence of 4.8 M urea to determine whether a particular amide proton exhibits EX1 or EX2 kinetics at this urea concentration (*41*, *46*). As shown in Figure 2, the observed rate constant is directly proportional to the deuterioxide concentration, so eq 4 predicts that the rate constant of an amide site exchanging by EX2 will increase by a factor of 5 in going from pH* 6.35 to 7.05. By contrast, an amide site exchanging by EX1 (see eq 3) contains no term that is pH dependent, so the rate constant will not change as a function of pH*. These predictions hold so long as the stability of the protein is pH* independent, as is the case here (see Table 1), and no conformational differences exist in the native state ensemble at the two pH* values. Thus, amide protons exchanging purely by EX1 in a plot of log k_{ex} at pH* 7.05 vs log k_{ex} at pH* 6.35 (see Figure 3) should fall on a diagonal line with a slope of one and intercept of zero. Those amide sites exchanging purely by EX2 are expected to fall on a line that is parallel to the diagonal line but displaced by an amount equal to the pH* difference of the two sets of measurements. According to these predictions, the experimental HX data obtained in Figure 3 cluster into three groupings: those that exhibit EX2 kinetics, those that fall between EX1 and EX2, and those exhibiting EX1 kinetics. Though there are a small number of exceptions, in the presence of 4.8 M urea most of the slowest exchanging amide protons (Figure 3a) are observed to exchange via EX1. Those exchanging at intermediate rates generally exchange by EX1 or a mixture of EX1 and EX2, and the fastest exchanging amide protons most often follow EX2 kinetics (Figure 3b). Because some rate constants are known with greater certainty than others, error bars are provided in Figure 3a,b. With the exception of two amides of the slow class, the combined data set in Figure 3c is shown without accompanying errors to enable easy visualization.

Hydrogen Exchange of RNase A in 0−*5.8 M Urea.* Among the 123 amide protons in RNase A, the exchange rate constants of only about a third can be evaluated using the quench method developed in an earlier study (*29*). All k_{ex} data for RNase A taken at pH* 6.35 in 0−5.8 M urea and pH* 7.05 in 4.8 M urea are listed in Table 2.

Within the (pre-denaturation) urea concentration range, where native RNase A represents essentially 100% of the protein, some amide protons exchange by way of EX1, some by EX2, and some by a mixture of EX1 and EX2 (see Figure 3). Accordingly, we have opted to display the kinetic data in a model-independent manner as shown in the figures that follow. For clarity in presentation, the rate constant data are divided into three categories, distinguished by their magnitudes and their dependence on urea concentration.

The first of the three classes is the slowest exchanging amide proton class. Not only do amide protons belonging to

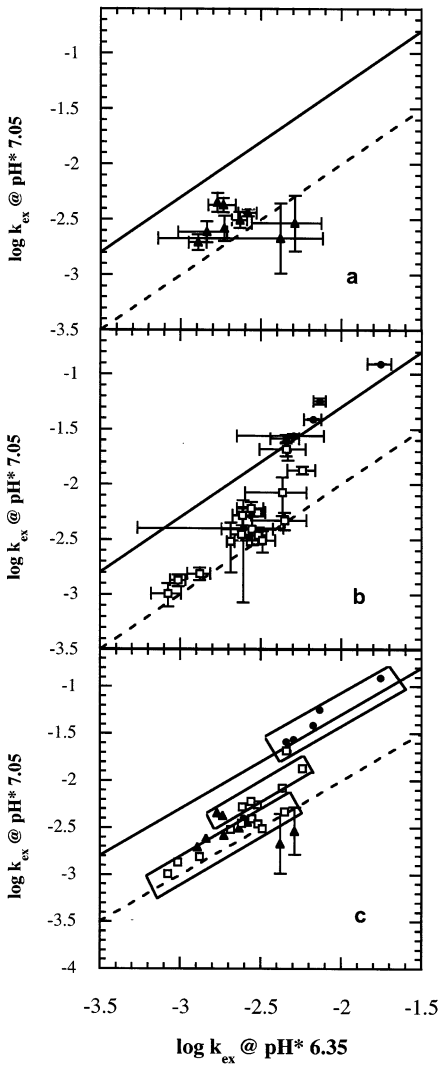

FIGURE 3: EX1/EX2 hydrogen exchange mechanism test of RNase A in 4.8 M urea at pH* 6.35 and 7.05. (a) Slow exchange amide proton class (filled diamonds). Rank order from slowest to fastest: V108, C58, V47, Y73, M79, I106, I81, Q74, E46. C58 and M79 have the largest error limits and are considered to be on the main diagonal. (b) Fast exchange amide proton class (filled circles). Rank order from slowest to fastest: N44, D14, Q60, K61, S59, V43, Y97. Intermediate exchange amide proton class (open squares). Slowest to fastest: V118, V116, I107, V63, H119, C84, K104, A56, H48, E49, C72, K98, Q11, M13, H12. (c) Composite plot of all exchange classes grouped in boxes according to the applicable HX mechanism that applies.: EX1 kinetics (box aligned with the dashed line), EX2 kinetics (box aligned with the solid line), and a mixture of EX1 and EX2 kinetics (box between the two lines). The dashed line represents the main diagonal, having a slope of unity and intercept of zero. The solid line has a slope of unity and intercept of 0.7.

this class have the smallest rate constants, the rate constants are also the most dependent on urea concentration of all the classes and the dependence is linear over a substantial urea concentration range. The slowest exchanging amide protons of RNase A are presented in Figure 4a, and the residues belonging to this class display large and similar slopes (0.79 $\pm$ 0.04) in the plot of log k_{ex} vs [urea]. Though the slopes of the lines in Figure 4a are quite similar, the parallel lines at any given urea concentration cover a 6−10 fold range in rate constant. The slowest amide protons in the presence of 4.8 M urea exchange primarily by EX1, though a small number exchange by a mixture of EX1 and EX2 (see Figure 3a).

Within the class of slowest exchanging amide protons, evaluation of k_{ex} data for [urea] < 1.9 M is neither practical nor accurate because exchange is so slow under these conditions. The bold solid lines in Figure 4a are provided for reference, and will be displayed in other plots to aid analysis and comparison of the hydrogen exchange data.

The second class of RNase A amide protons are the fastest exchanging amide protons measured. The rate constants for this class are all greater than 10^{-3} min^{-1} and all are considered to be independent of urea concentration over a range of at least 0−5 M. Only when [urea] exceeds 5 M, and the denaturation transition zone is entered, do these residues begin to show a rate constant increase trend (see Figure 4b). The urea concentration-independent exchange behavior of these amide protons suggest they are exchanging from the native ensemble by means of local structural fluctuations. According to the results of the EX2/EX1 test provided in Figure 3b, all but one of the residues in the fast class exchange by the EX2 mechanism in 4.8 M urea.

The third and final class of amide exchange sites are the intermediate exchange amide protons whose rate constants fall between the fast and slowest classes of amide exchange sites (see Figure 4c). In 4.8 M urea, these residues exchange by EX1 or by a mixture of EX1 and EX2. At low urea concentration, the intermediate exchange amide protons exhibit little or no dependence on urea concentration. However, with increased denaturant concentration, the rate constants become increasingly dependent on urea concentration, ultimately merging into the same urea rate constant dependence observed for the slowest class of RNase A amide protons.

Apparent Superprotection Appears If Exchange Is Analyzed by Means of EX2. In many kinetic studies exchange by EX2 is assumed to occur in the pH range of 6 to 7 at 25 °C, and frequently the data are analyzed assuming this mechanism (*47*, *48*). The EX2 mechanism provides information on the equilibrium constant involved in solvent exposure of the exchangeable site, and evaluation of these equilibrium constants using eq 6 provides data for a plot of ΔG_{HX} versus urea concentration. At high urea concentration, such a plot (not shown) of our data gives ΔG_{HX} values for some of the amide protons within the fast and intermediate classes that appear to be more protected than the amide protons of the slowest class. Such paradoxical behavior has been reported in the literature and is known as "superprotection" (*42*). In the present case, apparent "superprotection" is seen because the EX2 model is inappropriate for amide protons exhibiting EX1 kinetics.

TMAO Decreases the HX Rate Constants of a Number of RNase A Exchangeable Sites. TMAO is known to shift the midpoint of equilibrium denaturation to higher urea concentration, so TMAO in the presence of urea is fully expected to significantly decrease the H/D exchange of amide protons in the transition zone. Of interest, however, is how 1 M TMAO affects urea-dependent rate constants of the various classes as a function of urea concentrations under which the native species is most prominent. Figure 5 gives a plot of the observed urea-dependent HX rate constants in the presence and absence of 1 M TMAO, and for the sake of reducing the volume of data, the behaviors of only a representative number of sites are presented. The data are for beta strand 5 (β-5) of RNase A, which is composed of residues from the fast (Y97 and C110), intermediate (K98

Table 2: Base 10 Log of HX Rate Constants of RNase A in 0−5.8 M Urea at pH* 6.35 and in 0 M Urea at pH* 7.05

	pH* 7.05	pH* 6.35								
AA#	4.8 M	0 M	1.0 M	1.9 M	2.9 M	3.4 M	3.9 M	4.8 M	5.3 M	5.8 M
9	−1.04				−2.29		−2.05		−1.50	−1.18
10		−2.67		−1.96		−2.27		−2.02		−1.41
11	−2.08	−3.71	−3.63	−2.96		−2.73	−2.47	−2.37	−2.23	−1.65
12	−1.68	−3.70	−3.25	−2.88	−2.81	−2.50	−2.34	−2.34	−1.95	−1.53
13	−1.87	−3.97	−3.49	−3.32	−2.97	−2.65	−2.60	−2.24	−2.06	−1.68
14	−1.69	−2.94		−2.40	−2.67	−2.24	−2.08	−2.33	−2.11	−1.59
29	−1.84	−2.49		−2.67	−2.59	−2.67			−2.15	−1.45
31		−1.57			−2.06	−1.63	−1.83	−1.94	−1.74	−1.40
43	−1.25	−1.79		−1.98	−2.09	−1.93	−1.96	−2.13	−2.08	−1.75
44	−2.40		−2.34	−2.65	−2.78	−2.82	−2.53	−2.61	−2.34	−1.46
46	−2.35			−4.90	−4.12	−3.44	−3.09	−2.77		−1.73
47	−2.61			−5.16	−4.29	−3.86	−3.34	−2.84	−2.46	−1.83
48	−2.33	−4.25	−4.11	−3.80	−3.55	−3.19	−2.84	−2.35	−2.27	−1.73
49	−2.28	−3.26			−3.37	−3.19	−2.72	−2.61	−2.49	−1.69
53	−1.38				−2.16	−1.98				−1.29
54	−2.75	−5.19	−5.11	−5.08	−4.66	−4.22	−3.71	−2.99	−2.60	−2.21
55				−4.38		−3.85	−2.99	−2.15	−2.18	−1.62
56	−2.41	−3.44	−3.33	−3.36	−3.23	−3.07	−3.17	−2.55	−2.22	−1.92
57	−2.39					−4.18	−3.59	−2.45		−1.80
58				−4.85	−3.95	−3.51	−3.11	−2.38	−2.34	−1.45
59	−1.41	−1.87		−2.30	−2.16	−1.98	−2.04	−2.17	−2.19	−1.71
60	−1.59	−2.49	−2.48	−2.50	−2.61	−2.38	−2.26	−2.34	−2.41	−1.52
61	−1.56	−1.63	−2.40		−2.31	−2.06	−2.33	−2.30	−2.17	
63	−2.52	−4.97	−4.91	−4.80	−4.16	−3.71	−3.27	−2.69	−2.45	−1.94
72	−2.26	−3.43	−3.38	−3.40	−3.46	−3.03	−2.89	−2.52	−2.33	−1.85
73	−2.58			−4.97	−3.92	−3.56	−3.09	−2.73	−2.29	−1.85
74	−2.37			−4.68	−3.87	−3.57	−3.11	−2.74		−1.65
79				−4.50		−3.15	−2.90	−2.29		−1.58
81	−2.44			−5.04	−4.06	−3.57	−3.12	−2.58	−2.41	−1.95
84	−2.46	−4.29	−4.33	−4.31	−3.78	−3.45	−3.04	−2.52	−2.28	−1.79
85			−3.28	−3.49	−3.66	−3.36	−3.05	−2.64	−2.37	−1.91
97	−0.91	−2.01			−1.95	−1.88	−1.89	−1.76	−1.94	−1.71
98	−2.22	−3.98	−3.97	−3.87	−3.65	−3.37	−3.01	−2.56	−2.35	−1.57
104	−2.45	−4.62	−4.45	−4.24	−3.78	−3.32	−3.00	−2.62	−2.36	−1.85
106	−2.51			−5.10	−4.12	−3.58	−3.17	−2.63	−2.34	−1.88
107	−2.81	−4.35	−4.39	−4.29	−4.38	−3.98	−3.52	−2.88	−2.72	−2.13
108	−2.71				−4.72	−4.28	−3.67	−2.89	−2.65	−2.20
109				−5.27	−4.46	−3.87		−2.79	−2.65	−2.09
110	−1.43	−1.95	−2.10	−2.20	−2.19	−2.19	−2.02		−2.00	−1.60
116	−2.87		−5.00	−4.75	−4.42	−4.24	−3.68	−3.01	−2.67	−2.13
118	−2.99		−5.07	−4.95	−4.52	−4.17	−3.78	−3.08	−2.73	−2.37
119	−2.51	−4.52	−4.46	−4.21	−3.55	−3.20	−2.84	−2.49	−2.22	−1.73

and K104), and slowest (A109) H/D exchange classes. TMAO exerts its greatest effect on the slowest exchanging amide protons (A109) at about 4 M urea, and becomes less effective as the urea:TMAO ratio increases further. The smallest effects by 1 M TMAO on HX rate constants occur with the fastest exchanging amide proton class in the absence of urea.

Figure 6a shows that in the absence of urea, 1 M TMAO has essentially no effect on HX of most of the fastest exchanging amide protons; only S59 shows a decrease in the HX rate constant in the presence of TMAO. In the presence of 4.8 M urea (Figure 6b), discernible effects by TMAO on the fast exchange sites are detectable but small.

Figure 7a shows HX rate constants of residues in the intermediate exchange class in the presence and absence of 1 M TMAO at pH* 6.35, and Figure 7b gives results of experiments conducted in the same fashion but with the additional presence of 4.8 M urea. In the absence of urea, there are a small number of detectable decreases in HX rate constants in the presence of TMAO alone, while all intermediate exchange residues in the presence of 4.8 M are decreased by 1 M TMAO. It is important to point out that in the absence of urea, the data of Neira et al. indicate that essentially all of these intermediate exchanging amide protons exchange via EX2 (*49*). However, in 4.8 M urea nearly all of these sites have switched to EX1 exchange (see Figure 3b). As a result of the differences in mechanisms for exchange, the key protein species affected by TMAO change dramatically in the presence and absence of 4.8 M urea. In principle then, for the slowest exchanging amide protons (Figure 4a) one might expect to see a slope change on transition from EX2 to EX1 as a function of urea concentration, particularly if the low urea concentration data are analyzed according to EX2. Unfortunately, HX rates of the slowest exchanging amide sites are impossibly slow at low urea concentration, and the lack of HX rate data does not allow the possibility of analyzing HX data at low urea.

Finally, Figure 8 presents data collected in 4.8 M urea concerning effects of 1 M TMAO on the HX rate constants of the slowest exchanging amide protons. Under these conditions, all these sites exchange by way of EX1 or a combination of EX1/EX2 (see Figure 3a). According to the two-process model, HX from the slowest exchanging amide protons is believed to involve exchange from the denatured

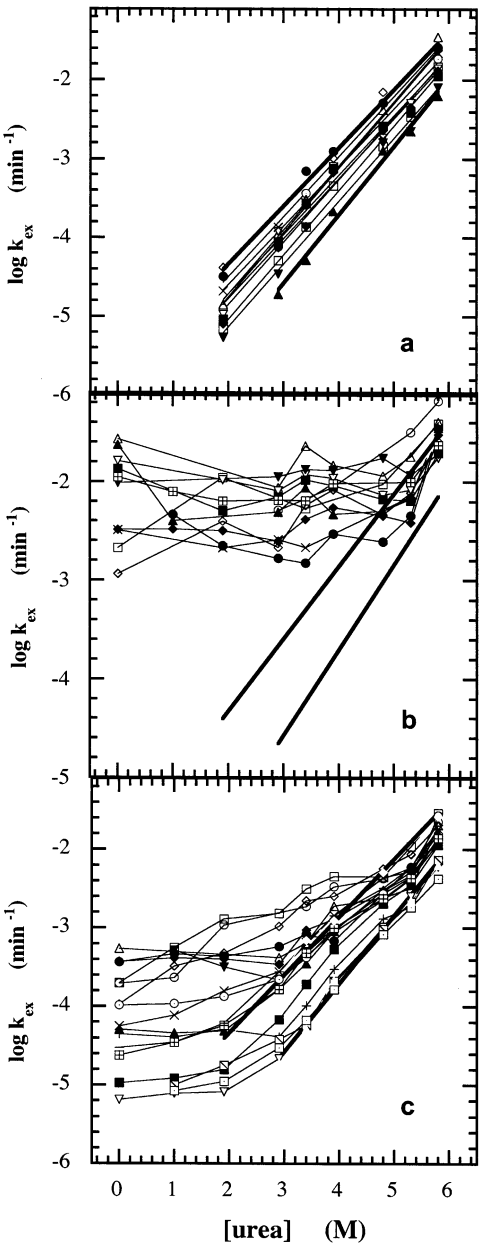

FIGURE 4: HX rate constants of amide exchange as a function of urea concentration. (a) HX rate constants of the slow exchange amide protons as a function of urea concentration. Thin lines represent the linear least squares best fits of rate constants as a function of urea concentration for the slow class of amide sites. The bold lines represent the approximate range of values within the slow class of amide sites and are included in subsequent panels for reference. F46, open circles; V47, open squares; Q55, open diamonds; C58, open up-triangles; Y73 open down-triangles; Q74, X; M79 filled circles; I81, filled squares; I106, filled diamonds; I108, filled up-triangles; A109, filled down-triangles. (b) HX rate constants of the fast exchange amide protons as a function of urea concentration. E9, open circles; R10, open squares; D14, open diamonds; M29, X; K31, open up-triangles; V43, open down-triangles; N44, filled circles; S59, filled squares; Q60, filled diamonds; K61, filled up-triangles; Y97, filled down-triangles; C110, open square with plus sign. (c) HX rate constants of the intermediate exchange amide protons as a function of urea concentration. Q11, open circles; H12, open squares; M13, open diamonds; H48, X; E49, open up-triangles; E54 open down-triangles; A56, filled circles; V63, filled squares; C74, filled diamonds; C84, filled up-triangles; R85, filled down-triangles; K98, open circle with dot; K104, open squares with plus sign; I107, plus sign; V116, open square with slash; V118 open square with dot; H119, minus sign.

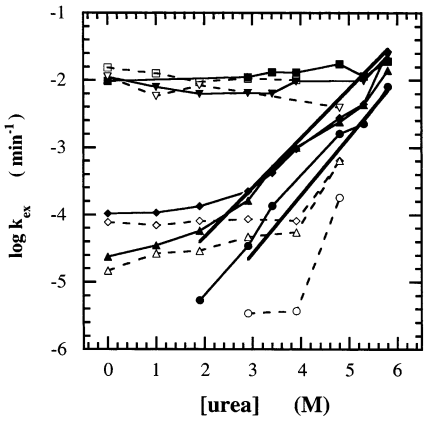

FIGURE 5: HX kinetic constants of the β5 strand of RNase A as a function of urea concentration. Bold lines bracketing the slowest exchange class of amide sites are provided for reference. The solid lines and filled points are data obtained in the presence of urea alone, while the dashed lines and open symbols represent rate constants obtained in the presence of 1 M TMAO at the urea concentration given. Y97, filled squares; C110, filled down-triangles; K98, filled diamonds; K104, filled up-triangles; A109, filled circles.

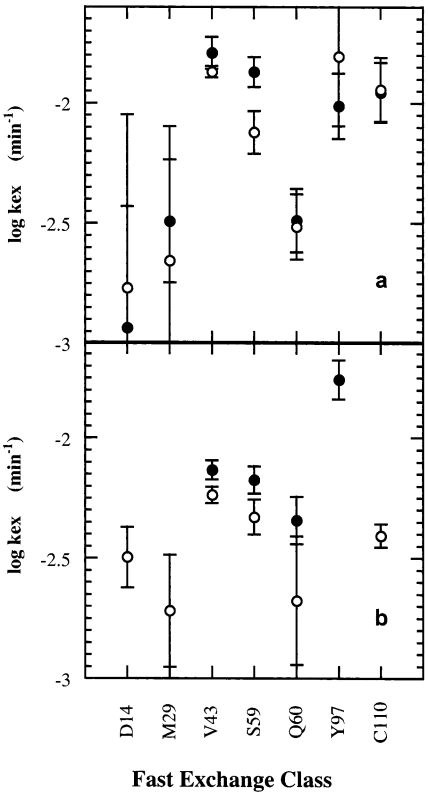

FIGURE 6: HX rate constant data for the fast exchange class of amide sites. (a) Rate constants taken in the absence (filled circles), and presence (open circles) of 1 M TMAO. (b) HX rate constant data for the fast exchange class taken in the presence of 4.8 M urea, with (open circles) and without (filled circles) 1 M TMAO. Missing points are due either to exchange becoming too fast for the quench method used, or for technical reasons involving the quench method.

state (*44*, *50*−*53*). Usually, this statement refers to the case in which EX2 kinetics is the dominant mechanism of exchange with the native state being "closed" and the denatured state as the "open" species. However, in our situation at high pre-denaturational concentrations of urea, EX1 kinetics prevails. Our view is that there are important

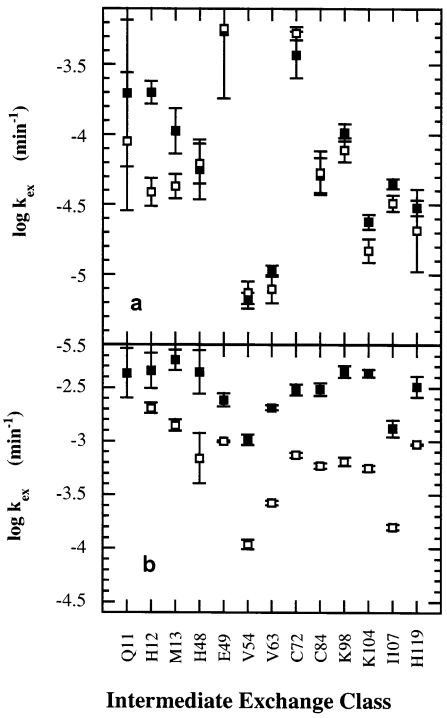

FIGURE 7: HX rate constant data for the intermediate exchange class of amide sites. (a) Rate constants taken in the absence (filled squares), and presence (open squares) of 1 M TMAO. (b) Rate constants taken in the presence of 4.8 M urea, with (open squares) and without (filled squares) 1 M TMAO.

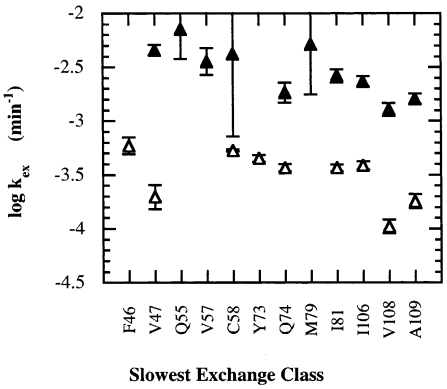

FIGURE 8: HX rate constant data for the slow exchange class of amide sites. Rate data were taken in the presence of 4.8 M urea, with (open triangles) and without (filled triangles) 1 M TMAO. Missing points are due to technical reasons involving the quench method.

similarities between EX1 and EX2 in this case, and key to these similarities is the description of the (EX1) activated complex as being much like a denatured species. For example, EX2 kinetics is considered to involve equilibrium between the closed form (native species) and the globally denatured form, while for EX1 kinetics, transition state theory invokes the concept of equilibrium between the closed form (native species) and the activated complex. Both EX1 and EX2 involve the closed (native state) species, and the extent to which the participating species are similar depends on how much the activated complex resembles a denatured protein. It is known that TMAO does not have much of an effect on the native state; its thermodynamic effect is on the denatured species, significantly raising its free energy in proportion to the degree of backbone exposure (*23*, *54*). Given that the TMAO greatly decreases the activation free energy of the EX1 sites in RNase A as would be expected of considerable backbone being exposed in the activated complex, and recalling that the activation free energy is a reflection of the equilibrium between the closed (native state) species and the activated complex, there is good reason to believe that the activated complex is structurally similar to denatured protein.

DISCUSSION

The cells of cartilaginous fishes are remarkable in that they contain the strong denaturant, urea, at intracellular concentrations that can affect structure and function of many proteins (*2*, *8*, *11*, *55*). The cells also contain TMAO, a protecting osmolyte that has the ability to counteract urea effects. TMAO and urea are both naturally occurring osmolytes, and their effects on protein structure and dynamics of proteins have direct bearing on their biological effects. In this study, using HX kinetics, we assess the effects of urea concentration on the dynamics of RNase A structural events resulting in proton exchange at specific amide sites in the protein. To understand urea's effects on the native ensemble, we have studied RNase A HX near neutral pH at urea concentrations spanning the pre-denaturation range (0−4.8 M urea, >99.5% native state) and extending a short distance into the transition zone (up to 5.8 M urea). Hydrogen exchange of RNase A in urea alone, in TMAO alone, and in urea:TMAO mixtures are discussed.

TMAO and, particularly, sucrose increase solvent viscosity. If viscosity plays a role in HX kinetics, it would be expected to affect HX rate constants in a manner inversely proportional to the relative viscosities of the osmolytes. With the exception of S59, one molar concentrations of neither urea, nor TMAO nor sucrose (*29*) have an affect on HX rate constants of the fast exchange sites of RNase A. The one exception is the HX rate constant of S59 in which TMAO decreases the rate constant, but neither 1 M urea nor 1 M sucrose has an effect. The general lack of effects of these osmolytes on the fast exchange class provides strong evidence that solution viscosity is not a factor of importance in HX from these sites. Rate constants of the slowest exchange amide sites in RNase A are decreased by 1 M concentrations of urea, TMAO, or sucrose, but to a much larger extent than can be accounted for by the relative viscosities (unpublished data) of these osmolytes. The decreases in HX rate constants of the slowest class of RNase A amide sites by these osmolytes are correlated with the osmophobic properties of the osmolyte, not their relative viscosities. From the observations involving fast and slow exchange sites, there is no evidence in support of viscosity is a factor of importance in RNase A HX kinetics.

As in other reported HX studies of proteins as a function of denaturant concentration, urea effects on RNase A HX rate constants can be grouped into three classes: (i) the slow exchange class (which has the strongest dependence on urea concentration), (ii) the fast exchange class (which exhibits essentially no dependence on urea concentration), and (iii) the intermediate exchange class (which exhibits little or no urea dependence at low urea concentration and strong dependence in high urea) (*48*). All of these characteristic dependencies are fully evident (Figure 4a−c) within the pre-denaturation urea concentration range (0−4.8 M). It is also

clear that, at the beginning of the N ↔ D equilibrium transition (5.8 M urea), the rate constants of all three classes converge to a narrow but significant range of rate constants, which have strong dependence on urea concentration.

Distinguishing EX1 Exchanging Amide Protons from EX2. An often used test to determine whether particular amide protons exchange via EX1 or EX2 involves plotting log k_{ex} values determined at one pH* vs log k_{ex} values obtained at a second pH* (*41*, *46*, *49*, *56*). The test purports to take advantage of the fact that amide protons exchanging by EX2 are directly dependent on pH* while those exchanging via EX1 are pH* independent. Because pH* dependence of k_{ex} can arise for reasons other than that explicit in the Hvidt and Nielsen general mechanism for HX, it is worthwhile discussing the test in some detail (*38*).

If one plots log k_{ex} values observed at some fixed pH*, say pH* 6.35 in our case, versus itself (i.e., log k_{ex} (6.35) vs log k_{ex} (6.35)), all rate constants will align along a diagonal with slope of one and intercept of zero. To obtain a plot as in Figure 3c, we now replace each rate constant on the ordinate with its corresponding log k_{ex} value obtained at a higher pH*, say pH* 7.05 in our case. Any movement of the points from the main diagonal can only be in the vertical direction. Following are four possible results one might obtain from such a plot.

(i) Vertical movement of points from the main diagonal may occur either because the stability of the protein is dependent on pH* or the native state conformation differs at the two pH* values (*38*). Alternatively, we may be in a pH* range where pK_a values of one or more ionizable groups are perturbed in the native ensemble, and this too will lead to pH*-dependent rate constants.

Rate constant dependence on pH* from these factors are not explicitly considered by the Hvidt and Nielsen mechanism for HX, and their appearance as pH*-dependent processes in the plot tend to obscure effects arising from the general HX mechanism. We have minimized these factors by showing in Table 1 that RNase A stability is unchanged between pH* 6.35 and 7.05, and that proton uptake or release is zero at pH 7.1 and small at pH 6.35 (*24*).

(ii) All amide protons exchanging via EX2 are predicted to be pH*-dependent and are expected to move vertically upward from the main diagonal by an amount equal to the difference between pH* 7.05 and 6.35 (*41*). In so doing, they will form a line parallel to the main diagonal with a slope of unity and a log k_{ex} (7.05) intercept of 0.7. All but one amide site (N44) of the fast exchange amide proton class (Figure 4b) are observed to follow this prediction (see Figure 3b,c).

(iii) In contrast to the EX2 sites, amide protons that are not affected by pH will remain on the main diagonal line (see Figure 3c). For such sites, the HX rate constant at pH* 7.05 is identical to that at pH* 6.35, and by definition these pH*-independent amide protons meet the criteria for EX1 exchange. In our case, seven of nine amide sites in the slowest exchange class, as well as several exchangeable protons in the intermediate class, can be classified as EX1 on this basis.

(iv) Clarke and Fersht claim that exchange sites involving slow rate constants that exchange via EX1 are manifested as a line with a slope of zero in the plot (*41*). To achieve such a result, several rate constants on the main diagonal at the lower pH* must increase to different extents at the higher pH*, achieving log k_{ex} values that are identical to one another at the higher pH*. Clearly, such sites cannot be pH*-independent, and on this basis they do not meet the test criteria set for EX1.

Nevertheless, rate constants that form a line with zero slope on the plot are to be classified as EX1 sites. The reason is that at the higher pH* the rate constants at these sites become identical, implying that they all exchange by global exposure to solvent. Thus, rate constants of amide sites that form a line of zero slope in such a test plot are EX1, despite the fact that they exhibit pH* dependence.

The Two Manifestations of EX1. There are two distinctly different ways EX1 sites can show up in the log k_{ex} (higher pH*) vs log k_{ex} (lower pH*) plot: (i) they can appear on the main diagonal line with slope of unity and zero intercept, or (ii) they can appear in the plot as a line with zero slope (*41*). The EX1 sites that are on the main diagonal are pH-independent, i.e., they exhibit EX1 kinetics at both the high and low pH* values, and the variation in magnitude of their rate constants along the main diagonal show that exchange at the EX1 sites is uncorrelated. Uncorrelated exchange in RNase A in our case is also corroborated by the fact that TMAO suppresses the rate constants of the EX1 sites to different degrees (see Figures 7 and 8), suggesting different amounts of backbone exposure in the respective activated complexes. Using other techniques, Robertson's lab has also shown uncorrelated exchange for some turkey ovomucoid third domain EX1 sites (*57*, *58*).

The second category of EX1 sites, the ones that should appear on the plot as a line with zero slope, are pH*-dependent and involve sites that at the lower pH* exchange in part or entirely by EX2, and shift to EX1 exchange at the higher pH*. The fact that such EX1 sites all exhibit the same HX rate constant suggests that their highly correlated exchange involves global unfolding. Robertson and colleagues have amply demonstrated such pH-induced conversion of EX2 sites to EX1 in the basic pH* range (*44*, *45*).

The slow exchange sites of barnase in low concentrations of guanidinium chloride exhibit this zero slope behavior, suggesting that EX2 to EX1 conversion of these sites at denaturant concentrations occurs prior to the onset of the denaturing transition of this protein (*59*). The results we have presented with RNase A shows that in pre-denaturational concentrations of urea EX2 to EX1 conversion occurs for all except the fast amide exchange class. In our case, the EX1 sites exhibit uncorrelated exchange while the EX1 sites in Barnase exhibit correlated exchange.

Basis for Interpreting Effects of Urea and TMAO on HX. In the Machino and Fridovich model, urea is said to shift the native ensemble to a more expanded average structure while TMAO contracts the native state ensemble. The native state is highly compact already, so contraction of this state by TMAO is meant to describe a decrease in amplitudes and/or numbers of native state fluctuations while expansion by urea is thought of as an increase in number and/or amplitudes of native state fluctuations. The point to be made is that in the vernacular of the Machino and Fridovich model, the terms expansion and contraction involve small changes that may not be sufficient to cause a native state dimension change detectable by current physical methods.

It is known that TMAO has an unfavorable interaction with the peptide backbone, and this behavior, called the osmophobic effect, is responsible for its biological role in stabilizing proteins in urea-rich cells (*23*, *54*). Relative to the native state, more backbone units are exposed in the denatured protein, and the osmophobic effect brought on by TMAO increases the Gibbs energy of the denatured state relative to that of native, thereby causing the N ↔ D equilibrium to shift in favor of the N state (*23*, *26*, *54*, *60*). Application of these principles to HX means that TMAO will suppress fluctuations that expose peptide backbone, causing HX rate constants to decrease, and the degree of suppression will be proportional to the additional amount of peptide backbone exposed in the structural fluctuation.

In contrast to TMAO, urea has a favorable interaction with the peptide backbone, causing a decrease in Gibbs energy of the denatured state relative to native, and a shift in the N ↔ D equilibrium in favor of the D state (*23*, *61*). Urea's favorable interaction with the peptide backbone promotes exposure of peptide backbone, increasing the HX rate constant in proportion to the additional amount of backbone exposed in the fluctuation (*61*). These opposing effects of TMAO and urea on protein stability are believed to be central to TMAO's counteraction of urea effects on protein function in urea-rich cells (*23*, *26*).

The urea:TMAO paradigm holds that urea should interact favorably with the backbone and side chains, making the native state less compact, and that TMAO will counteract these effects. In terms of HX, native state expansion by urea would be expected to increase the amplitudes and frequencies of native state fluctuations, and TMAO should suppress them. Given that the slowest sites require the largest exposure of peptide surface area for exchange while the fast exchange sites require much less exposure of surface area, a strong correlation is expected between the ability of TMAO to suppress exchange at sites and the rank order of their exchange rates. In the presence of 4.8 M urea, this prediction is born out in that the rate constants of slowest exchange sites are suppressed the most by (1 M) TMAO (Figure 8), less by the intermediate (Figure 7b), and least by the fast exchange sites (Figure 6b). The magnitude of the suppression by TMAO shown here would be greater if the 4.8:1 ratio of urea:TMAO in this experiment was closer to 2:1 as found in living organisms (*8*).

Effects of Urea and/or TMAO on Native State Exchange. Several lines of evidence point to the conclusion that urea dramatically affects HX of RNase A at pre-denaturational concentrations of urea, and that TMAO counteracts urea's effects. Figure 4a−c shows that in the absence of either osmolyte, rate constants for exchange cover several orders of magnitude, and this range narrows to around 1 order of magnitude in 4.8 M urea. Over this urea concentration range, the native population remains at >99.5%, and the mechanism for exchange goes from being almost exclusively EX2 to largely EX1. At the very least, these conditions promote the view of a protein whose structure becomes increasingly perturbed by the increasing urea concentration, allowing increased opportunistic binding of urea to the exposed protein segments as fluctuation amplitudes get larger and more frequent. Over this urea concentration range, TMAO is shown (Figures 7 and 8) to oppose urea's effects on structural fluctuations. Taken together, the results provide reasonable support for the concept that urea causes increases in the frequency and amplitudes of structural fluctuations, causing the average structure of the predominant protein species (>99.5% native) apparently to expand somewhat as urea concentration is raised from zero to 4.8 M. The fluctuations contributing to the apparent expansion are both local (native state) and global (denatured state), with the large amplitude (global) fluctuations primarily responsible for the greatest degree of expansion. Unfortunately, it is the fluctuations from the native state that are most closely allied with function, so the important question is not whether expansion and/or contraction can be established for the principal protein species within the experimental conditions, but whether evidence of "expansion" by urea and "contraction" by TMAO can be established for exchange from the native state ensemble.

It is important then to establish criteria for determining which HX sites exchange from the native ensemble. In pH* 6.35 buffer solution, HX occurs by way of EX2 for RNase A (*49*). As mentioned, the two-process model involves native state hydrogen exchange occurring by way of local fluctuations, and by global unfolding involving exchange from the denatured state (*50*−*53*). For any given amide site, the fraction of HX contributed by local (native state) fluctuations can be estimated from the fact that the observed rate constant is the sum of contributions by the two processes and from knowledge of the rate constant for HX extrapolated from high denaturant concentration to the zero denaturant limit. By way of example, E54 is the slowest exchanging member of the intermediate class and is a site most likely to have measurable exchange via the urea-dependent process most evident at high urea concentration. At >3 M urea, E54 exchanges entirely by EX1, and extrapolation of the urea-dependent behavior in the 3−5.8 M range to zero denaturant gives E54's EX1 exchange rate constant in pH 6.35 buffer. The observed rate constant for E54 in the absence of urea and/or TMAO is found to be 97-fold faster than E54's EX1 exchange rate constant, and calculation shows that in buffer 99% of HX from this site occurs by way of local exchange from the native state ensemble. For intermediate and fast exchange amide sites, all of which exchange faster than E54, local (native state) fluctuations overwhelmingly dominate EX1 contributions. Thus, in buffer local (native state) EX2 describes the mode of exchange from the intermediate and fast class of amide sides in RNase A.

Evidence for all aspects of the urea:TMAO paradigm requires attention to the separate effects of low urea and low TMAO concentration on the native state ensemble. In the field of hydrogen exchange, the general consensus is that exchange from the native state largely involves solvent penetration events or local unfolding, i.e., events involving little exposure of peptide backbone. This consensus is justified by the observation that exchange rate constants of a large number of sites exhibit little or no dependence on urea at low denaturant concentration. Because urea and TMAO require exposure of peptide backbone to exert their effects, HX occurring with little increase in backbone exposure immediately creates problems in trying to study the effects of these osmolytes on the native state ensemble. Fortunately, not all amide sites exchanging from the native state are independent of urea concentration, and some examples of these sites have been of particular interest as possible indicators of intermediate states in protein folding.

By way of example, denaturant-dependent native state exchangeable sites described as partially unfolded forms (PUFs) have been reported (*62*−*64*), and clear identification of an unfolded segment of a PUF in a mutant form of apocytochrome b562 has been demonstrated (*65*).

The fact remains that although they can be important in studies of native state dynamics, denaturant-dependent HX sites are in the minority at low urea, giving the appearance that urea does not seem to have extensive influence on fluctuations involving the native ensemble. With this issue in mind, the possibility has recently been raised that urea does have significant effects on the native ensemble, but the effects are masked because of a peculiar property of native state EX2 exchange. Simulations of native state fluctuations involving as much as 10−20% of surface area exposed on denaturation have been shown to exhibit hydrogen exchange rate constants that appear to be independent of urea concentration (*66*). The reason cited is that the ensembles that comprise "open" and "closed" states involved in (local) EX2 exchange are very similar in terms of the degree of surface area exposure. With the same area exposed, urea should interact to the same extent with both states, resulting in no shift of the "closed" to "open"equilibrium and consequently no observed effect of urea on EX2 kinetics. In such cases, even if urea expanded the "closed" and "open" forms by increasing the fluctuations of both states, these effects on the native ensemble would go undetected by HX kinetics because with both forms being expanded to the same extent would be no shift in the "closed" to "open" equilibrium (*66*). In lieu of a difference in surface area exposed for the "closed" and "open" ensembles, TMAO would also not shift the "closed" to "open"equilibrium. That is, despite the fact that TMAO might diminish the putative 10−20% backbone exposure resulting from fluctuations, its effects would also not be detected by EX2 HX kinetics. The point to be made from the work of Wooll et al. is that the very nature of the native ensemble and the EX2 mechanism can mitigate against detection of important urea (or TMAO) effects on the native ensemble.

Given the various conditions that mitigate against observing effects of urea or TMAO on native state hydrogen exchange, it is significant whenever evidence is found for the influence of effects by these agents on native state exchange. Figures 6a and 7a show that one molar TMAO in pH* 6.35 buffered RNase A solution decreases the observed HX rate constants of S59, H12, M13, K104, and I107; the largest effects are on sites with the largest rate constants (S59, H12, M13). These five intermediate and fast exchange amide sites are a subset of twenty such fast and intermediate exchange sites whose kinetics we have been able to monitor in pH* 6.35 buffered RNase A. As in the example involving E54 (see above), the residues of the fast and intermediate exchange classes exchange by local (native state) fluctuations. Thus, in buffer alone TMAO is seen to decrease the rate constants for native state exchange of 15−25% of all the intermediate and fast amide sites whose kinetics we have been able to observe. While it is clear that TMAO does not affect the rate constants of all sites exchanging by fluctuations of the native ensemble, it does suppress fluctuations of a significant fraction of those sites in a manner consistent with Machino and Fridovich's concept of "contraction" of the native state ensemble.

We take these results as evidence that, by itself, TMAO suppresses RNase A native state hydrogen exchange at a number of sites and that the same sites whose rate constants are increased by urea in low urea concentration (H12, K104, and M13) are also affected by TMAO. TMAO can also suppress HX rate constants at sites (S59 and I107) that exhibit no urea dependence. Why TMAO appears to affect more sites than does urea may be related to the fact that, on a per mole basis, TMAO has twice the effect on function as does urea (*8*). The demonstrated ability that TMAO and urea can separately and oppositely affect rate constants for native state exchange provides evidence for that part of the urea:TMAO paradigm relating ensemble behavior to opposing effects of these naturally occurring osmolytes.

The counteracting ability of TMAO on protein function has prompted the search for effects of TMAO on the native states of proteins, and while some studies have failed to show effects on protein dynamics, others have reported success. In an interesting report, Jaravine et al. show opposing effects of both urea and TMAO on HX kinetics at four sites on the relatively unstable cold shock protein A (CspA) (*56*). However, application of the above-described EX1/EX2 test to their data reveals no sites that can be classified strictly as EX2, and given the low stability of the protein and its fast folding and unfolding rate constants, it is not entirely clear whether exchange at these sites is occurring from the native or the denatured state. Results of another study claim effects of TMAO on RNase A at pH* 4, but the results are not readily interpretable due to TMAO being a salt (pK_a of TMAO is 4.75) at the pH* of the measurement (*67*). It is known that the thermodynamic character of native RNase is greatly perturbed by salt at this pH, so it is probable that the effects observed are a result of a salt effect rather than a protecting osmolyte effect on the native ensemble (*24*, *68*).

In contrast to the two reports mentioned above, Gonnelli and Strambini failed to detect effects by TMAO on the internal dynamics of native proteins. These authors monitored tryptophan phosphorescence of several proteins in the presence and absence of TMAO as a means of detecting effects of TMAO on the native state ensemble (*69*). The authors claim that tryptophan phosphorescence is very sensitive to local environment and the lack of effects of TMAO on tryptophan phosphorescence in the enzymes studied was interpreted to mean that osmolytes do not affect the internal dynamics of the native state (*69*).

The extent to which osmolytes affect native state internal dynamics may depend on the dynamical characteristics under observation. For example, we have shown that amide proton exchange from histidine 119 of RNase A is quite slow with exchange occurring from the denatured ensemble. By contrast, recent NMR spin relaxation measurements suggest chemical exchange between conformers at multiple backbone sites including His119 occurs on the millisecond time scale (*70*). Clearly, the dynamical character of the backbone at any given site depends on what measure of dynamics is under consideration, and failure to detect effects in one measure of dynamics may not preclude success in detecting effects by other measurements. Our objective in the present study was to use HX as a monitor of native state dynamics in investigating the essential aspects of the urea:TMAO paradigm and evidence is presented in support of observing

opposing effects of urea and TMAO alone and in combination. There may indeed be other measures of native state dynamical character more responsive to urea and TMAO effects than HX; application of other methods of observing dynamics would be valuable in pursuing this problem further.

From the current study and those mentioned above, it is clear that demonstrating effects of urea and TMAO on the native ensembles of proteins is difficult, requiring attention to multiple issues that can affect the interpretation. The work presented here provides results in support of the urea:TMAO paradigm which posits that TMAO and urea have opposing effects on the amplitudes and frequency of protein fluctuations, with urea tending to increase fluctuations and TMAO suppressing them. These effects are readily evident with HX from the denatured state, but not as evident for HX from the native ensemble. When both urea and TMAO are in the presence of protein the affects of both osmolytes appear to be additive, with TMAO counteracting the effects of urea on native state ensemble fluctuations.

ACKNOWLEDGMENT

The authors acknowledge helpful discussions with Drs. Andrew Robertson and Clare Woodward. We also thank the Sealy Center for Structural Biology for use of NMR equipment and facilities, and Dr. Shan Min Zhang for help in some technical aspects of the work.

REFERENCES

1. Hochachka, P. W., and Somero, G. N. (2002) *Biochemical Adaptation*, Oxford University Press, New York.
2. Yancey, P. H., Clark, M. E., Hand, S. C., Bowlus, R. D., and Somero, G. N. (1982) Living with water stress: evolution of osmolyte systems. *Science 217*, 1214−22.
3. Brown, A. D., and Simpson, J. R. (1972) Water Relations of Sugar-tolerant Yeasts: the Role of Intracellular Polyols. *J. Gen. Microbiol. 72*, 589−591.
4. Borowitzka, L. J., and Brown, A. D. (1974) The salt relations of marine and halophilic species of the unicellular green alga. *Dunaliella*: The role of glycerol as a compatible solute. *Arch. Microbiol. 96*, 37−52.
5. Bowlus, R. D., and Somero, G. N. (1979) Solute compatibility with enzyme function and structure: rationales for the selection of osmotic agents and end-products of anaerobic metabolism in marine invertebrates. *J. Exp. Zool. 208*, 137−51.
6. Pollard, A., and Wyn Jones, R. G. (1979) Enzyme Activities in Concentrated Solutions of Glycinebetaine and Other Solutes. *Planta 144*, 291−298.
7. Wang, A., and Bolen, D. W. (1996) Effect of proline on lactate dehydrogenase activity: Testing the generality and scope of the compatibility paradigm. *Biophys. J. 71*, 2117−2122.
8. Yancey, P. H., and Somero, G. N. (1979) Counteraction of urea destabilization of protein structure by methylamine osmoregulatory compounds of elasmobranch fishes. *Biochem. J. 183*, 317−323.
9. Bagnasco, S., Balaban, R., Fales, H. M., Yang, Y. M., and Burg, M. (1986) Predominant osmotically active organic solutes in rat and rabbit renal medullas. *J. Biol. Chem. 261*, 5872−7.
10. Yancey, P. H. (1985) in *Transport Processes, Iono- and Osmoregulation* (Gilles, R., and Gilles-Baillien, M., Eds.) pp 424−436, Springer-Verlag, Berlin Heidelberg.
11. Yancey, P. H., and Somero, G. N. (1980) Methylamine osmoregulatory solutes of elasmobranch fishes counteract urea inhibition of enzymes. *J. Exp. Zool. 212*, 205−213.
12. Garcia-Perez, A., and Burg, M. B. (1990) Importance of Organic Osmolytes for Osmoregulation by Renal Medullary Cells. *Hypertension 16*, 595−602.
13. Nakanishi, T., Uyama, O., Nakahama, H., Takamitsu, Y., and Sugita, M. (1993) Determinants of relative amounts of medullary organic osmolytes: effects of NaCl and urea differ. *Am. J. Physiol. 264*, F472−F479.
14. Yancey, P. H. (1988) Osmotic effectors in kidneys of xeric and mesic rodents: corticomedullary distributions and changes with water availability. *J. Comp. Physiol. B 158*, 369−380.
15. Somero, G. N. (1986) From dogfish to dogs: Trimethylamines protect proteins from urea. *News Physiol. Sci. 1*, 9−12.
16. Burg, M. B., Kwon, E. D., and Peters, E. M. (1996) Glycerophosphocholine and betaine counteract the effect of urea on pyruvate kinase. *Kidney Int. 50*, S1−S5.
17. Baskakov, I., Wang, A., and Bolen, D. W. (1998) Trimethylamine-*N*-oxide counteracts urea effects on rabbit muscle lactate dehydrogenase function: a test of the counteraction hypothesis. *Biophys. J. 74*, 2666−73.
18. Yancey, P. H. (1994) in *Cellular and Molecular Physiology of Cell Volume Regulation* (Strange, K., Ed.) pp 81−109, CRC Press, Ann Arbor.
19. Mashino, T., and Fridovich, I. (1987) Effects of urea and trimethylamine-*N*-oxide on enzyme activity and stability. *Arch. Biochem. Biophys. 258*, 356−360.
20. Burg, M. B., and Peters, E. M. (1997) Urea and methylamines have similar effects on aldose reductase activity. *Am. J. Physiol. 276*, F1048−53.
21. Gandour, R. D., and Schowen, R. L. (1978) Transitional States of Biological Processes, Plenum Press, New York.
22. Lumry, R., and Biltonen, R. (1969) in *Structure and Stability of Biological Macromolecules* (Timasheff, S., and Fasman, G., Eds.) pp 65−212, Marcel Dekker, New York.
23. Bolen, D. W., and Baskakov, I. V. (2001) The osmophobic effect: natural selection of a thermodynamic force in protein folding. *J. Mol. Biol. 310*, 955−63.
24. Yao, M., and Bolen, D. W. (1995) How Valid Are Denaturant-induced Unfolding Free Energy Measurements? Level of Conformance to Common Assumptions over an Extended Range of Ribonuclease A Stability. *Biochemistry 34*, 3771−3779.
25. Pace, C. N. (1986) in *Enzyme Structure, Part L* (Hirs, C. H. W., and Timasheff, S. N., Eds.) pp 266−280, Academic Press, Inc.
26. Wang, A., and Bolen, D. W. (1997) A naturally occurring protective system in urea-rich cells: mechanism of osmolyte protection of proteins against urea denaturation. *Biochemistry 36*, 9101−8.
27. Means, G. E., and Feeney, R. E. (1971) *Chemical Modification of Proteins*, Holden-Day, Inc., San Francisco.
28. Stark, G. (1965) *Biochemistry 4*, 1030−1036.
29. Wang, A., Robertson, A. D., and Bolen, D. W. (1995) Effects of a naturally occurring compatible osmolyte on the internal dynamics of ribonuclease A. *Biochemistry 34*, 15096−15104.
30. Rico, M., Santoro, J., Gonzalez, C., Neira, J. L., Nieto, J. L., and Herranz, J. (1989) Sequential H NMR assignment and solution structure of bovine pancreatic ribonuclease A. *Eur. J. Biochem. 183*, 623−638.
31. Robertson, A. D., Purisima, E. O., Eastman, M. A., and Scheraga, H. A. (1989) Proton NMR Assignments and Regular Backbone Structure of Bovine Pancreatic Ribonuclease A in Aqueous Solution. *Biochemistry 28*, 5930−5938.
32. O'Neil, J. D. J., and Sykes, B. D. (1989) NMR studies of the influence of dodecyl sulfate on the amide hydrogen exchange kinetics of a micelle-solubilized hydrophobic tripeptide. *Biochemistry 28*, 699−707.
33. Forsen, S., and Hoffman, R. A. (1963) Study of moderately rapid chemical exchange reactions by means of nuclear magnetic double resonance. *J. Chem. Phys. 39*, 2892−2901.
34. Dempsey, C. E. (1986) pH dependence of HX from backbone peptide amides in Apamin. *Biochemistry 25*, 3904−3911.
35. Santoro, M. M., and Bolen, D. W. (1988) Unfolding Free Energy Changes Determined by the Linear Extrapolation Method. 1. Unfolding of Phenylmethanesulfonyl α-Chymotrypsin Using Different Denaturants. *Biochemistry 27*, 8063−8068.
36. Englander, S., and Kallenbach, N. (1983) *Q. Rev. Biophys. 16*, 521−655.
37. Loftus, D., Gbenle, G. O., Kim, P. S., and Baldwin, R. L. (1986) Effects of denaturants on amide proton exchange rates: a test for structure in protein fragments and folding intermediates. *Biochemistry 25*, 1428−36.
38. Hvidt, A., and Nielsen, S. O. (1966) Hydrogen exchange in proteins. *Adv. Protein Chem. 21*, 287−386.
39. Bai, Y., Milne, J. S., Mayne, L., and Englander, S. W. (1993) Primary Structure Effects on Peptide Group Hydrogen Exchange. *Proteins: Struct., Funct., Genet. 17*, 75−86.
40. Kim, K.-S., Fuchs, J. A., and Woodward, C. K. (1993) Hydrogen Exchange Identifies Native-State Motional domains Important in Protein Folding. *Biochemistry 32*, 9600−9608.

41. Clarke, J., and Fersht, A. R. (1996) An evaluation of the use of hydrogen exchange at equilibrium to probe intermediates on the protein folding pathway. *Folding Des. 1*, 243−254.
42. Swint-Kruse, L., and Robertson, A. D. (1996) Temperature and pH dependences of hydrogen exchange and global stability for ovomucoid third domain. *Biochemistry 35*, 171−80.
43. Fuentes, E. J., and Wand, A. J. (1998) Local dynamics and stability of apocytochrome b562 examined by hydrogen exchange. *Biochemistry 37*, 3687−98.
44. Arrington, C. B., and Robertson, A. D. (1997) Microsecond protein folding kinetics from native-state hydrogen exchange. *Biochemistry 36*, 8686−91.
45. Sivaraman, T., Arrington, C. B., and Robertson, A. D. (2001) Kinetics of unfolding and folding from amide hydrogen exchange in native ubiquitin. *Nat. Struct. Biol. 8*, 331−3.
46. Skelton, N. J., Kordel, J., Akke, M., and Chazin, W. J. (1992) Nuclear magnetic resonance studies of the internal dynamics in Apo, (Cd2+)1 and (Ca2+)2 calbindin D9k. The rates of amide proton exchange with solvent. *J. Mol. Biol. 227*, 1100−17.
47. Bai, Y., Milne, J. S., Mayne, L., and Englander, S. W. (1994) Protein Stability Parameters Measured by Hydrogen Exchange. *Proteins: Struct., Funct., Genet. 20*, 4−14.
48. Mayo, S. L., and Baldwin, R. L. (1993) Guanidinium chloride induction of partial unfolding in amide proton exchange in RNase A. *Science 262*, 873−876.
49. Neira, J. L., Sevilla, P., Menendez, M., Bruix, M., and Rico, M. (1999) Hydrogen exchange in ribonuclease A and ribonuclease S: evidence for residual structure in the unfolded state under native conditions. *J. Mol. Biol. 285*, 627−43.
50. Woodward, C., and Hilton, B. (1980) Hydrogen isotope exchange kinetics of single protons in Bovine pancreatic trypsin inhibitor. *Biophys. J. 32*, 561−576.
51. Woodward, C., Simon, I., and Tuchsen, E. (1982) Hydrogen exchange rates and the dynamic structure of proteins. *Mol. Cell Biochem. 48*, 135−160.
52. Qian, H., Mayo, S. L., and Morton, A. (1994) Protein Hydrogen Exchange in Denaturant: Quantitative Analysis by a Two-Process Model. *Biochemistry 33*, 8167−8171.
53. Loh, S. N., Rohl, C. A., Kiefhaber, T., and Baldwin, R. L. (1996) A general two-process model describes the hydrogen exchange behavior of RNase A in unfolding conditions. *Proc. Natl. Acad. Sci. U.S.A. 93*, 1982−7.
54. Liu, Y., and Bolen, D. W. (1995) The peptide backbone plays a dominant role in protein stabilization by naturally occurring osmolytes. *Biochemistry 34*, 12884−12891.
55. Yancey, P. H., and Somero, G. N. (1978) Urea-Requiring Lactate Dehydrogenases of Marine Elasmobranch Fishes. *J. Comp. Physiol. 125*, 135−141.
56. Jaravine, V. A., Rathgeb-Szabo, K., and Alexandrescu, A. T. (2000) Microscopic stability of cold shock protein A examined by NMR native state hydrogen exchange as a function of urea and trimethylamine N- oxide. *Protein Sci. 9*, 290−301.
57. Arrington, C. B., Teesch, L. M., and Robertson, A. D. (1999) Defining protein ensembles with native-state NH exchange: kinetics of interconversion and cooperative units from combined NMR and MS analysis. *J. Mol. Biol. 285*, 1265−75.
58. Arrington, C. B., and Robertson, A. D. (2000) Correlated motions in native proteins from MS analysis of NH exchange: evidence for a manifold of unfolding reactions in ovomucoid third domain. *J. Mol. Biol. 300*, 221−32.
59. Clarke, J., and Fersht, A. R. (1996) An evaluation of the use of hydrogen exchange at equilibrium to probe intermediates on the protein folding pathway. *Fold Des. 1*, 243−54.
60. Baskakov, I., and Bolen, D. W. (1998) Forcing thermodynamically unfolded proteins to fold. *J. Biol. Chem. 273*, 4831−4.
61. Qu, Y., Bolen, C. L., and Bolen, D. W. (1998) Osmolyte-driven contraction of a random coil protein. *Proc. Natl. Acad. Sci. U.S.A. 95*, 9268−73.
62. Rumbley, J., Hoang, L., Mayne, L., and Englander, S. W. (2001) An amino acid code for protein folding. *Proc. Natl. Acad. Sci. U.S.A. 98*, 105−12.
63. Raschke, T. M., and Marqusee, S. (1998) Hydrogen exchange studies of protein structure. *Curr. Opin. Biotechnol. 9*, 80−6.
64. Bai, Y., Sosnick, T. R., Mayne, L., and Englander, S. W. (1995) Protein folding intermediates: Native-state hydrogen exchange. *Science 269*, 192−197.
65. Takei, J., Pei, W., Vu, D., and Bai, Y. (2002) Populating partially unfolded forms by hydrogen exchange-directed protein engineering. *Biochemistry 41*, 12308−12.
66. Wooll, J. O., Wrabl, J. O., and Hilser, V. J. (2000) Ensemble modulation as an origin of denaturant-independent hydrogen exchange in proteins. *J. Mol. Biol. 301*, 247−56.
67. Palmer, H. R., Bedford, J. J., Leader, J. P., and Smith, R. A. (2000) 31P and 1H NMR studies of the effect of the counteracting osmolyte trimethylamine-*N*-oxide on interactions of urea with ribonuclease A. *J. Biol. Chem. 275*, 27708−11.
68. Bolen, D. W., and Yang, M. (2000) Effects of guanidine hydrochloride on the proton inventory of proteins: implications on interpretations of protein stability. *Biochemistry 39*, 15208−16.
69. Gonnelli, M., and Strambini, G. B. (2001) No effect of trimethylamine *N*-oxide on the internal dynamics of the protein native fold. *Biophys. Chem. 89*, 77−85.
70. Cole, R., and Loria, J. P. (2002) Evidence for flexibility in the function of ribonuclease A. *Biochemistry 41*, 6072−81.

BI0206457